Taylor & Francis
Taylor & Francis Group

RESEARCH ARTICLE

Isolation, characterization, and *in silico*, *in vitro* and *in vivo* antiulcer studies of isoimperatorin crystallized from *Ostericum koreanum*

Hussain Raza[a], Qamar Abbas[a], Mubashir Hassan[a], Seong-Hui Eo[a], Zaman Ashraf[a], Daeyoung Kim[b], Abdul Rehman Phull[a], Song Ja Kim[a], Sung Kwon Kang[b] and Sung-Yum Seo[a]

[a]Department of Biological Sciences College of Natural Sciences, Kongju National University, Gongju, Chungnam, Republic of Korea;
[b]Department of Chemistry, Chungnam National University, Daejeon, Republic of Korea

ABSTRACT

Context: *Ostericum koreanum* (Maxim.) Kitagawa (Apiaceae) roots are traditionally used as an analgesic and antiulcer agent. However, the antiulcer potential of isoimperatorin isolated from *O. koreanum* has not yet been explored.

Aim: To evaluate the antiulcer activity of isoimperatorin isolated from the roots of *O. koreanum*.

Materials and methods: Isoimperatorin was isolated as cubic crystals by repeated column chromatography of the ethyl acetate fraction and structure was verified with ^{1}H NMR, ^{13}C NMR and high-resolution mass spectrometry (HRMS-FAB). The crystals obtained were analyzed with the single crystal X-ray method. The MTT assay was used to determine its cytotoxicity against chondrocytes at different concentrations (0.0–737.74 μM, 24 h). The *in vivo* antiulcer activity of isoimperatorin (40 mg/kg) was determined against ethanol-, indomethacin- and pyloric ligation-induced ulcers in Sprague-Dawley rats. Furthermore, the effect of isoimperatorin (0.0–737.74 μM, 24 h) on the expression of type II collagen in chondrocytes was determined using western blot method. The *in vitro* urease inhibitory activity of isoimperatorin (0–80 μM) and molecular docking was also performed against urease.

Results and discussion: Isoimperatorin demonstrated significant inhibitory activity (IC$_{50}$ 36.43 μM) against urease as compared to the standard drug thiourea (IC$_{50}$ 33.57 μM) without cytotoxic effects. It provided 70.9%, 67.65% and 54.25% protection in ulcer models induced by ethanol, indomethacin and pyloric ligation, respectively. Isoimperatorin showed the highest expression level of type II collagen at 368.87 μM. The docking results confirmed strong binding affinity with the target protein.

Conclusion: Isoimperatorin may be used to develop antiulcer drugs with decreased side effects.

Introduction

Gastric ulcers are an important disease of the digestive system and affect 5–10% of the adult population. They have become a global problem due to their higher morbidity and mortality, as well as their medical, social and economic impact (Bucciarelli et al. 2010; Ji et al. 2012). The complete pathophysiology is still not fully understood; probable aetiologies include an imbalance between protective factors of the gastric mucosal membrane (i.e., mucus and bicarbonate secretion) and aggressive factors (i.e., acid and pepsin secretion) (Ramakrishnan & Salinas 2007; de Souza Almeida et al. 2011). Several endogenous factors such as prostaglandin E2 (PGE2), somatostatin, nitric oxide (NO) and sulfhydryl compounds are involved in the pathophysiology of gastroprotection (Tsukimi et al. 2001). *Helicobacter pylori*, genetic factors, alcoholic beverages and the use of non-steroidal anti-inflammatory drugs (NSAIDs) are the main contributing factors for gastric ulceration (Konturek et al. 2005). Antacids, anticholinergics, proton pump inhibitors and histamine H2-receptor antagonists are drugs currently used for the treatment (Santin et al. 2010; Ji et al. 2012); however, they cannot be tolerated in the long-term because of their safety profile. Thus, medicinal plants have become attractive options for the development of newer agents due to their lower side effects (Sumbul et al. 2011).

Urease catalyzes the hydrolysis of urea to ammonia and carbamate, which is the final step in the nitrogen metabolism of organisms (Mobley & Hausinger 1989; Karplus et al. 1997). The rapid decomposition of carbamate yields a second molecule of ammonia. A significant increase in pH and the number of ammonium ions may occur due to these reactions; they are responsible for the negative effects of urease activity in humans. Urease is the main cause of urinary tract and gastrointestinal infections, and the latter may lead to severe pathologies such as peptic and stomach ulcer disease as in the case of *H. pylori*. As ureases are involved in ulcer pathophysiology in humans and animals, urease inhibitors have been considered models for the development of new antiulcer drugs (Ramsay et al. 2012).

Gastric ulcers occur due to inflammation of the stomach lining after damage to the epithelial cells of the mucosa (Fatima et al. 2008). The process of mucosal or other wound healing involves a complex cascade of events, comprising the coordination of different cellular activities such as the chemotaxis and synthesis of extracellular matrix components (Adam et al. 1999).

Collagen is the major protein of the extracellular matrix and an essential component of the wound-healing process after ulceration, which involves the crosslinking of collagen and remodelling of tissue; therefore the organization of this protein is crucial in the healing process (Hermes et al. 2013).

Recently, herbal compounds have played an important role in the discovery and development of modern drugs against ulcers and other diseases due to their potentially improved safety and efficacy over conventional treatments. *Ostericum koreanum* (Maxim) Kitagawa (Apiaceae) is a popular oriental medicine in Korea, and its crude extracts are widely used as analgesic agent (Yun et al. 2003). Its roots are traditionally used for gastrointestinal disorders. There have been no reports on antiulcer activity of isoimperatorin isolated from the roots of *O. koreanum* in the current literature. Therefore, the present study assessed the antiulcer activity of the compound with the aim of developing a safe and effective drug for treating gastric ulcers.

Materials and methods

Plant material

The dried roots of *O. koreanum* were purchased from the Korean Collection of Herbal Extracts, a biotech company in Korea, during May 2015. Plant material was verified by Professor Young-Han You, Department of Biology, Kongju National University, Republic of Korea. A voucher specimen was kept in our laboratory for future reference.

Extraction and fractionation

The plant material (shade dried, 5 kg) was mixed with methanol (20 L) and kept for one week at room temperature. The mixture was stirred with a glass rod once daily. The obtained extract was then filtered and evaporated under reduced pressure using a rotary evaporator (Eyela Rotary Vacuum Evaporator N-N- series, Japan) at 40 °C to yield an extract (600.5 g). The crude MeOH extract was then suspended in distilled water (3 L) in a separating funnel, and subsequently partitioned with *n*-hexane (3 L × 3), ethyl acetate (3 L × 5), dichloromethane (3 L × 1), and *n*-butanol (3 L × 3), leaving an aqueous fraction. The fractions were evaporated under reduced pressure to yield fractions of *n*-hexane (150.8 g), ethyl acetate (260.9 g), dichloromethane (0.0 g) and *n*-butanol (45.2 g).

Isolation of compound

Based on the activity-guided fractionation method, the ethyl acetate soluble fraction (26.1 g) was applied to a silica gel column (6id ×350 mm, 1000 mL, 24/40) and eluted with a gradient from n-hexane to ethyl acetate to yield 30 subfractions (E1-E30). Subfractions E1-E20 (9.5 g) were combined based on their thin-layer chromatography (TLC) profile. The combined subtractions were applied to a silica gel column (3.5id ×350 mm, 500 mL, 24/40) and eluted with a gradient from *n*-hexane to ethyl acetate. The compound was crystallized at 9:1 of *n*-hexane and ethyl acetate. Reverse phase HPLC was performed to assure the purity of the isolated compound by using MeOH and H_2O (4:1 and 1:1) as an eluent on a reverse phase C18 column (Young Lin Instrument co, Korea).

Characterization

^{1}H NMR, ^{13}C NMR and mass (HRMS FAB) spectroscopic techniques were used to verify the final structure of the isolated compound. ^{1}H NMR and ^{13}C NMR spectra were recorded on a Bruker 400 MHz spectrometer using $CDCl_3$ as a solvent. A DFS (Thermo Scientific, Germany) instrument was used to analyze the HRMS (FAB). Single crystal X-ray analyses were carried out using the Bruker instrument (SMART CCD area-detector diffractometer). The melting point was recorded using Digimelt (MPA-160, USA Melting Point Apparatus).

Urease inhibition assay

Urease inhibitory activity was determined via methods detailed by Weatherburn (1967) and Rafiq et al. (2012) with few modifications. Briefly, 40 μL of buffer (100 mM urea, 0.01 M K_2HPO_4, 1 mM EDTA and 0.01 M LiCl; pH 8.2), 20 μL of enzyme (5 U/mL) and 10 μL of isoimperatorin were mixed in a 96-well plate and incubated at 37 °C for 30 min. Subsequently, 40 μL of phenol reagent (1% w/v phenol and 0.005% w/v sodium nitroprusside) and 40 μL of alkali reagent (0.5% w/v NaOH and 0.1% active chloride NaOCl) were added into each well. The plate was then incubated for 35 min at room temperature, and absorbance was measured at 625 nm using a microplate reader (Optimax Tunable, Sunnyvale, CA). Thiourea was used as a reference in this study. All reactions were performed in triplicate and repeated thrice. Inhibition was calculated using the following equation:

$$\text{Inhibition} (\%) = [(B{-}S)/B] \times 100$$

B and *S* are the absorbances for the blank and the samples, respectively.

IC_{50} values were calculated using Prism 5.0 (GraphPad, San Diego, CA).

Cytotoxicity and collagen expression analysis

Antibodies and chemicals

Dulbecco's modified Eagle's medium (DMEM) and foetal bovine serum (FBS) were purchased from Invitrogen (Burlington, Ontario, Canada). Collagenase types II, streptomycin, penicillin and dimethylsulfoxide (DMSO) were from Sigma-Aldrich (St. Louis, MO). All antibodies against Type II collagen and GAPDH were purchased from Santa Cruz Biotechnology Inc. (Santa Cruz, CA).

Cell culture

Rabbit articular chondrocytes were isolated from the cartilage of 2-week-old New Zealand white rabbits (Koatech, Pyeongtaek-si, Gyeonggi-do, Korea). Cartilage slices were dissociated enzymatically for 8 h in 0.2% collagenase type II (381 units/mL) in DMEM. Individual cells were obtained by collecting the supernatant after brief centrifugation. The cells were suspended in DMEM supplemented with 10% (v/v) FBS, 50 μg/mL streptomycin and 50 units/mL penicillin, before being plated in culture dishes at a density of 2×10^5 cells/cm^2. The media were changed every 2 days after seeding, with cells reaching confluence after approximately 3 days. Afterwards, the cells were treated with various concentrations (0.0–737.74 μM) of isoimperatorin for 24 h. Chondrocytes cells were treated with 368.87 μM isoimperatorin and 10 ng/mL IL-1β for 24 h, or pre-stimulated with 368.87 μM isoimperatorin alone for 1 h before being co-treated with isoimperatorin and 10 ng/mL IL-1β for 24 h. Cell cultures were grown in an incubator (Sanyo, Osaka, Japan) at 37 °C in a

humidified atmosphere containing 5% CO_2. Study protocol was approved by the Institutional Review Board of Kongju National University (IRB No. 2011-2).

Cell viability assay

MTT assay was used to quantify the viability of cells treated with isoimperatorin. Chondrocytes were seeded in 96-well plates at a density of 1×10^4 cells/well and cultured for 24 h before treatment with isoimperatorin. Next, 10 µL/well of MTT reagent 1 (methylthiazole tetrazolium, 10 mg/mL) was added to the cells and the plate was incubated for 4 h at 37 °C until purple formazan crystals developed. This was followed by the addition of 100 µL MTT reagent 2 (solubilization buffer, 10% SDS with 0.01 N HCl, DMSO) in every well. The absorbance was measured at 600 nm by using a microplate reader (OPTI$_{Max}$ Tunable, Sunnyvale, CA) after incubation overnight. Each treatment was performed in quadruplicate.

Western blot analysis

Proteins were isolated in cold radioimmunoprecipitation assay (RIPA) buffer (50 mM Tris-HCl, pH 7.4, 150 mM NaCl, 1% NP-40, 0.1% SDS, supplemented with phosphatase inhibitors and protease inhibitors); equal amounts of total cellular proteins were resolved by SDS-PAGE. The resolved proteins were transferred to nitrocellulose membranes, which were blocked with 5% non-fat dry milk for 1 h before incubating with primary antibodies overnight at 4 °C. After washing, blots were developed using peroxidase-conjugated secondary antibodies and visualized using an ECL detection system (BioFact^{TM}).

Animal experiments

Animals and maintenance

Healthy adult male Sprague-Dawley rats (average body weight, 180 ± 10 g) were obtained from Daehan Biolink Co. (Chungcheongbuk-Do, Korea). Rats were maintained under controlled environmental conditions: temperature, 25 ± 3 °C; 12 h light/dark cycle; free access to food and water *ad libitum*. After the animals adapted to their laboratory conditions for 1 week, they were randomly distributed into groups. All animals used in the current study were treated humanely according to the 'Principles of Laboratory Animal Care,' and the guidelines provided by the local ethics committee of the Department of Biology Kongju National University, Gongju, Republic of Korea, on the human use of animals for scientific research.

Dose selection

In our initial trial experiments, isoimperatorin at different dosages (10, 20 and 40 mg/kg of animal body weight) in DMSO were administered. All three concentrations were administered before exposure to the ulcerogen. From these experiments, significant results were found at a concentration of 40 mg isoimperatorin/kg of body weight (bw); subsequently, this concentration was selected for further study.

Ethanol-induced ulcer

After 16 h of fasting, the Sprague-Dawley rats were divided into different groups ($n = 5$). The control group received only distilled water. The second group received only ethanol, and served as the ethanol-induced ulcer control. In the third group, isoimperatorin was orally administered at the concentration of 40 mg/kg bw, and 30 min later, absolute ethanol (1 mL/200 g bw) was administered orally (Awaad et al. 2015). Animals were sacrificed at 1 h after ethanol administration. The stomach was then removed and cut along the greater curvature to observe the gastric lesions.

Indomethacin-induced ulcer

Antiulcer activity was also determined in an indomethacin-induced ulcer model previously reported by Djahanguiri (1968) with some modification. All fasted rats were treated with the vehicle and 40 mg/kg of isoimperatorin (orally). After 1 h, animals were orally administered 50 mg/kg indomethacin (dissolved in 2% $NaHCO_3$). After 4 h, the animals were sacrificed, and the stomachs were removed and opened for observation.

Pylorus ligation-induced ulcer

Ulcers were induced by ligating the pylorus according to the method previously reported by Shay (1945). Fasted rats were treated orally with the vehicle and 40 mg isoimperatorin/kg bw. During experimentation, food was removed from the cages. Thirty minutes after compound administration, the animals were anaesthetized with anesthetic ether. The abdomen was opened and stomach was slightly lifted out and ligated with care to avoid any injury or damage to the veins. The stomach was carefully replaced and the wound was closed. The animals were allowed to recover with free access to water. Four hours after ligation, the animals were sacrificed and stomachs were removed for ulcer observation.

Ulcer measurement

Ulcer size was determined via the following arbitrary scoring system (Srivastava et al. 1991):

(I)	shedding of epithelium	10
(II)	petechial and frank haemorrhages	20
(III)	one or two ulcers	30
(IV)	more than two ulcers	40
(V)	perforated ulcers	50

Percent inhibition was determined according to the formula:

$$\text{Percent inhibition} = \frac{\text{Ulcerated area (Ulcer control)} - \text{Ulcerated area (treated)}}{\text{Ulcerated area (Ulcer control)}} \times 100$$

Statistical analysis

Results are expressed as the mean ± the standard error. These values were calculated from the specified number of determinations. The data were tested for overall significance with an analysis of variance (ANOVA). A value of $p < 0.05$ was considered statistically significant.

In silico *analysis*

Retrieval of protein structure

The crystal structure of urease from jack bean was retrieved from the Protein Data Bank (PDBID 3LA4). The overall stereochemical properties and Ramachandran graph/values of urease were assessed using the Molprobity server (Lovell et al. 2003; Chen et al. 2009).

Ligand structure

The structure of isoimperatorin was minimized using the UCSF Chimera 1.10.1 molecular visualizing software (Pettersen et al. 2004) (Figure 1). Different online tools and servers such as Molinspiration (http://www.molinspiration.com/), Molsoft (http://www.molsoft.com/) and Osiris Property Explorer (http://cheminformatics.ch/propertyExplorer/) were employed to evaluate the chemoinformatics and drug-likeness properties of isoimperatorin. The Osiris Property Explorer (http://www.organic-chemistry.org/) was used to determine possible tumourigenic or mutagenic risks and to estimate the drug-like properties of the compound. Furthermore, pkCSM (http://bleoberis.bioc.cam.ac.uk/pkcsm/) was employed to predict its Absorption, Distribution, Metabolism, Excretion and Toxicity (ADMET) properties (Pires et al. 2015). The number of rotatable bonds including H-bond acceptors (HBA) and H-bond donors (HBD) were obtained using PubChem (https://pubchem.ncbi.nlm.nih.gov/). Similarly, other molecular properties such as molar refractivity, density, surface tension and polarizability were accessed by ChemSketch (http://www.acdlabs.com/resources/freeware/chemsketch/). Lipinski's rule of five was analyzed using Molsoft (http://www.molsoft.com/) and Molinspiraion (http://www.molinspiration.com/) online tools. The isoimperatorin was further used in docking analysis to identify its binding energy and residual interactions.

Molecular docking

A molecular docking study was performed using the Autodock 1.5.6 (Morris et al. 2009) docking tool to obtain different docking complexes of isoimperatorin against jack bean urease. The parameter values for the grid box were adjusted to attain the best binding conformation between isoimperatorin and the target protein. The parametric grid values for the urease protein were adjusted using specific centre coordinates ($X = 260.523$, $Y = 96.180$ and $Z = 2.4308$) with a spacing of 1.0 Å. The maximum number of docking poses (100 runs) was adjusted to obtain the best docking complex with the highest binding affinity. Docking analysis and visualization were carried out using Discovery Studio (2.1.0) (Studio D 2008) and UCSF Chimera 1.10.1, respectively.

Results and discussions

The methanolic extract of the roots of *O. koreanum* was partitioned into *n*-hexane, ethyl acetate, dichloromethane, *n*-butanol and aqueous fractions. Repeated column chromatographic purification of the ethyl acetate fraction led to the isolation of isoimperatorin.

Characterization

Chemical shifts (δ) are reported in ppm downfield from the internal standard, tetramethylsilane (TMS). The exact mass of the isoimperatorin was determined by HRMS analyses on a DFS high-resolution magnetic sector mass spectrometer. Fast atom bombardment (FAB) was used for ionization.

Isoimperatorin: white cubic crystals: (Figure 1); m.p: 107–109 °C; ^{1}H NMR (CDCl$_3$, δ ppm): 8.19 (d, $J = 9.2$ Hz, 1H, H-4), 7.61 (d, $J = 2.0$ Hz, 1H, H-2′), 7.17 (s, 1H, H-8), 6.97 (d, $J = 2.4$, 1H, H-3′), 6.30 (d, $J = 9.6$ Hz, 1H, H-3), 5.55 (m, 1H, H-2″), 4.94 (d, $J = 6.8$ Hz, 2H, H-1″), 1.82 (s, 3H, H-4″), 1.72 (s, 3H, H-5″); ^{13}C NMR (CDCl$_3$, δ ppm): 161.3 (C-2), 158.1 (C-7), 152.6 (C-5), 148.9 (C-9), 144.9 (C-2′), 139.8 (C-10), 139.5 (C-3″), 119.1 (C-2″), 114.2 (C-3), 112.5 (C-3′), 107.5 (C-4), 105.0 (C-8), 94.2 (C-6), 69.7 (C-1″), 25.8 (C-4″), 18.2 (C-5″); HRMS: *m/z* calculated for C$_{16}$H$_{15}$O$_4$: 271.0964: found: 271.0965 (Supplementary material). The isoimperatorin was recrystallized as cubic white single crystals suitable for single crystal analysis. The crystal showed triclinic $P\overline{1}$ space group, with the following other parameters: $a = 6.82$ Å $b = 8.50$ Å $c = 12.69$ Å, $\alpha = 94.39°$ $\beta = 103.97°$ $\gamma = 106.64°$. Figure 2 shows the ortep view of the crystal structure of isoimperatorin. After analyzing the cell parameters of the crystal, we cross-referenced it in Cambridge crystal database system and found that it exactly matched the reported crystal structure of isoimperatorin (Rajnikant Gupta et al. 1996).
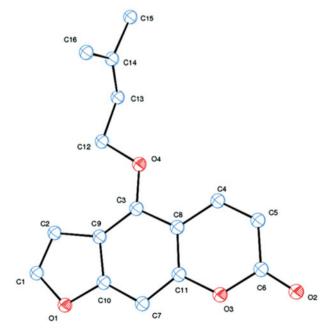

Figure 1. Chemical structure of isoimperatorin.

Figure 2. Ortep view of the crystal structure of isoimperatorin.

In vitro *urease inhibition*

The isolated compound isoimperatorin showed good jack bean urease inhibitory activity (IC_{50} 36.43 μM) as compared to the reference drug (IC_{50} 33.57 μM). It is well-known that the urease of *H. pylori* protects the microorganism in the stomach's acidic environment by converting urea into ammonia. One possible approach to treating *H. pylori* infections is to control the action of urease by using urease inhibitors (Awaad et al. 2015). Based on our results, isoimperatorin is a potential agent for antiulcer drug development.

Antiulcer activity on animals

In order to check the *in vivo* antiulcer activity of isoimperatorin, various models such as the ethanol-, indomethacin- and pyloric ligation-induced ulcers were used.

Ethanol-induced ulcer

Isoimperatorin showed significant antiulcer activity against the ethanol-induced ulcer (70.9% protection, $p < 0.001$, Figure 3). Gastric damage due to ethanol induction critically involves the generation of reactive oxygen species (Sidahmed et al. 2013). Ethanol is also known to decrease endogenous nitric oxide concentration in the gastric mucosa (Masuda et al. 1995). Nitric oxide is known to be an important defence mediator in the gastric mucosa (Brzozowski et al. 2006). The gastric mucosa is known to be the first line of defence in the stomach against harmful agents (Sidahmed et al. 2013).

Indomethacin-induced ulcer

The antiulcer potential of isoimperatorin was observed against indomethacin-treated rats, where the efficacy of isolated
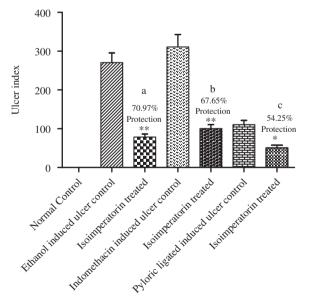

Figure 3. Effect of isoimperatorin on ulcer index for ulcers induced by ethanol, indomethacin, or pylorus ligation. Numbers indicate the % protection with respect to the control groups of different ulcer models. Bars represent the mean ± SEM of each group ($n = 5$). One-way analysis of variance (ANOVA) was employed and significant differences between control groups and groups treated with isoimperatorin are represented by *$p < 0.05$ and **$p < 0.001$. (a) % protection of isoimperatorin in ethanol-induced ulcer model (b) % protection of isoimperatorin in indomethacin induced ulcer model (c) % protection of isoimperatorin in pyloric ligated induced ulcer model

compounds was observed to be 67.65% ($p < 0.01$, Figure 3). The non-steroidal anti-inflammatory drug indomethacin is known to increase the risk of upper gastrointestinal haemorrhages and gastric ulcer (Wolfe et al. 1999; Ray et al. 2007). Prostaglandins play a vital protective role by maintaining the blood flow of the mucosa and by stimulating the secretion of bicarbonate and mucus, which are responsible for mucosal cell renewal. Non-steroidal anti-inflammatory drugs suppress prostaglandin and increase the risk of gastric lesions (Malfertheiner et al. 2009). In the present study, isoimperatorin significantly reduced mucosal haemorrhages in the indomethacin-induced ulcer model, indicating the possible involvement of prostaglandins in its antiulcer activity.

Pylorus ligation-induced ulcer

The antiulcer activity of isoimperatorin was also observed against the pyloric ligation-induced ulcer model in rats (54.25% protection, $p < 0.05$). In this ulcer model, the self-digestion of the mucosa by gastric acid results in ulcer development (Figure 3) (Goel & Bhattacharya 1991).

After comparison of all three ulcer models, isoimperatorin was found to best protect against ulcer development in the ethanol-induced ulcer model, suggesting that it may protect the gastric mucosa by mediating endogenous nitric acid levels.

Cell viability assay

The MTT assay is significant in the assessment of cell apoptosis. Rabbit chondrocytes were cultured after treatment with 0.0–737.74 μM isoimperatorin for 24 h. The cells treated with 0.0, 36.88, 92.21, 184.43, 368.87 and 737.74 μM isoimperatorin did not show statistically significant differences in cell viability (Figure 4(a)). The results confirmed that isoimperatorin treatment had no effects on proliferation and apoptosis in rabbit articular chondrocytes, and indicated that isoimperatorin did not show signs of toxicity to the cells (Figure 4(b)).

Effect of isoimperatorin on collagen expression

Collagens play important roles in wound healing and are thought to contribute to the structural support and framework of healing that includes cell differentiation, migration and synthesis of important proteins (Brett 2008). Different concentrations of isoimperatorin (0.0–737.74 μM) were tested on rabbit articular chondrocytes, and western blot analysis was performed to determine its effect on the expression of type II collagen. It was observed that the expression levels of type II collagen gradually increased and highest expression was found at 368.87 μM (Figure 5(a)). The expression was further confirmed in the presence of IL-1β, isoimperatorin up-regulated the expression of type II collagen which is down-regulated by IL-1β (Figure 5(b)). Wound healing in ulcers is marked by the initial replacement of the mucosal defects and the migration of epithelial cells that are supported by a meshwork of connective tissues. The extracellular matrix plays a key role in wound healing by providing support to the regenerating cells. The distribution of intestinal collagens in both the mucosa and normal gastric tissue in humans thus reduces gastric ulcer (Gillessen et al. 1993). This indicates the significance of collagen as the main element in thick fibrils for the support and structural stability of damaged mucosa. Collagen formation is activated not only in the submucosa but also in deeper layers such as the muscularis propria and serosa.
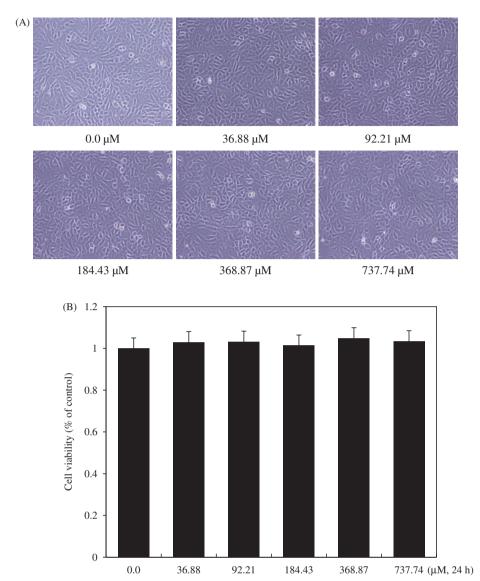
(A)

0.0 μM   36.88 μM   92.21 μM

184.43 μM   368.87 μM   737.74 μM

(B)

Figure 4. Effect of isoimperatorin treatment on the viability of rabbit articular chondrocytes. Chondrocytes were treated with the indicated concentrations (0.0–737.74 μM) of isoimperatorin for 24 h. Photographs of chondrocytes (A) were taken with a phase-contrast microscope (200× magnification). Cell viability was estimated using the methyl thiazole tetrazolium (MTT) assay. The graphical data (B) are expressed as mean ± standard error of mean.
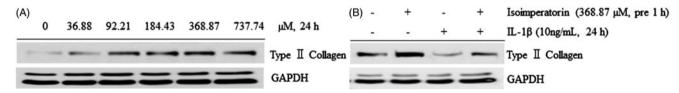

Figure 5. Effect of isoimperatorin on the dose-dependent expression of type II collagen in primary chondrocytes. After the treatment of chondrocytes with indicated concentrations of isoimperatorin for 24 h, (A) type II collagen expression was detected using Western blot analysis. (B) Isoimperatorin increased the expression of type II collagen in primary chondrocytes in the presence or absence of IL-1β. GAPDH was used as the loading control.

This reflects the synchronized interaction of all structural layers of the gastric wall during the gastric ulcer-healing process (Shahin et al. 1997).

In silico study

Jack bean urease and structural assessment

Jack bean urease is a hydrolase enzyme, and consists of a single chain of 840 amino acid residues. The secondary structure of this protein consists of 29% α helices and 22% β sheets (Kabsch & Sander 1983). The X-ray diffraction study confirmed the following: resolution, 2.05 Å; R-value, 0.183; unit cell crystal dimensions, $a = 138.57$ Å, $b = 138.57$ Å, $c = 198.35$ Å; angles, $\alpha = 90°$, $\beta = 90°$ and $\gamma = 120°$. The reliability and stability of the structure of urease was confirmed by Ramachandran plots (Lovell et al. 2003), which indicated that 99.9% of all residues were in the allowed region (>99.8%, Figure 6). The only outlier (HIS 545) was observed in the structural assessment. The urease Ramachandran graph and their predicted values showed good
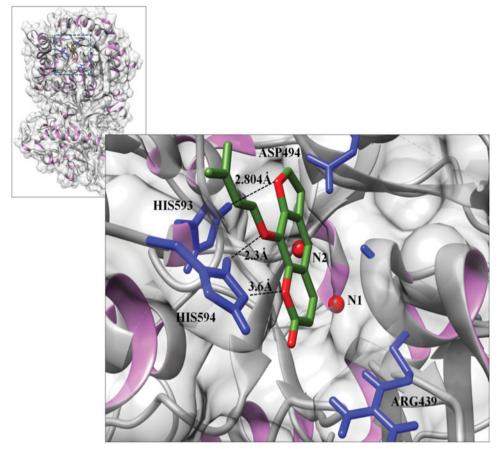
Figure 6. Interactions between isoimperatorin and Jack bean urease (PDB ID 3LA4) at the active site, generated using Discovery studio 2.1.0. The light silver colour shows the backbone of the urease protein in solid ribbon format. Carbon and oxygen atoms of the ligand molecule are shown in green and red, respectively. The interacting residues are shown in blue, while the dotted lines indicate the binding distances (Å).

accuracy of phi (φ) and psi (ψ) angles among the coordinates, with most of residues in the acceptable region.

Ligand evaluation

Computational analysis of the isolated ligand molecule (Figure 1) predicted their chemo-informatics and ADMET (Absorption, Distribution, Metabolism, Excretion, and Toxicity) properties (Table 1 and 2). The predicted properties absorption, water solubility, intestinal solubility and skin permeability suggested that the isolated compound has strong potential as drug. Similarly, the predicted blood–brain barrier (BBB) and central nervous system permeability values (0.117 and −1.793, respectively) are comparable with standard values (0.3 and −2) (Pires et al. 2015). These predicted values confirmed its therapeutic potential in targeting the urease protein. Additionally, the predicted values of metabolism, excretion and toxicity also confirmed its drug-likeness behaviour. Negligible Ames toxicity and low oral rat acute toxicity (LD_{50}) values (2.229) also enhance its potential as a good pharmaceutical agent, as does its negative hepatotoxicity and skin sensitization property, which indicate little harm after use of the compound. Predicted chemoinformatic properties such as Log$P$, Log$S$, hydrogen bond donor (HBD), hydrogen bond acceptor (HBA), molar volume (Mol.Vol), density, polarizability, surface tension and drug-likeness values of the isolated molecule further suggest good drug-like behaviour. Lipinski's rule of five also confirmed its therapeutic potential against the respective target molecule.

Table 1. Chemo-informatic properties of isoimperatorin.

Chemo-informatics properties	Values
Molecular formula	$C_{16}H_{14}O_4$
Molecular weight	270.27996
Composition	C (71.10%) H (5.22%) O (23.68%)
Molar refractivity	75.01 ± 0.03 cm^3
Molar volume	217.4 ± 3.0 cm^3
Parachor	568.5 ± 6.0 cm^3
Index of refraction	1.606 ± 0.0
Surface tension	46.7 ± 3.0 dyne/cm
Density	1.242 ± 0.06 g/cm^3
Polarizability	$29.73 \pm 0.5 \ 10^{-24}$ cm^3
Monoisotopic mass	270.089209 Da
Number of HBA	4
Number of HBD	0
MolLogP	3.84
MolLogS	3.00
MolPSA	36.35 A^2
MolVol	297.81 A^3
Number of stereo centres	0
Drug-Likeness model score	−0.73
Lipinski rule	Yes

HBA: hydrogen bond acceptor; HBD: hydrogen bond donor.

Binding conformation and docking analysis of isolated compound

The conformational binding analysis of the isolated compound against urease is shown in Figure 6. The compound–urease docking complex provides information on the conformational state of candidate molecules with the best-fitted pose, along with hydrogen bonding (H-bonds) pattern. Our isolated compound fits in a

Table 2. ADMET properties of isoimperatorin.

Property	Model name	Predicted values	Units
Absorption	Water solubility	−4.433	(log mol/L)
	Caco2 permeability	1.365	(log Papp in 10^{-6} cm/s)
	Intestinal absorption (human)	97.293	(% Absorbed)
	Skin permeability	−2.673	(log Kp)
	P-glycoprotein substrate	Yes	(Yes/No)
Distribution	VDss (human)	−0.23	(log L/kg)
	Fraction unbound (human)	0.18	(Fu)[a]
	BBB permeability	0.117	(log BB)[b]
	CNS permeability	−1.793	(log PS)[c]
Metabolism	CYP2D6 substrate	No	(Yes/No)
	CYP1A2 inhibitor	No	(Yes/No)
	CYP3A4 inhibitor	Yes	(Yes/No)
Excretion	Total clearance	0.968	(log mL/min/kg)
	Renal OCT2 substrate	No	(Yes/No)
Toxicity	Ames toxicity	No	(Yes/No)
	Maximum tolerated dose (human)	0.979	(log mg/kg/day)
	Oral rat acute toxicity (LD_{50})	2.229	(log mg/kg_bw/day)
	Hepatotoxicity	No	(Yes/No)
	Skin sensitization	No	(Yes/No)

ADMET: Absorption, Distribution, Metabolism, Excretion and Toxicity.
[a]fu, fraction unbound in plasma.
[b]Log BB, Blood–brain barrier;.
[c](Log PS), rate of passive diffusion/permeability; brain/plasma equilibration rate.

Table 3. Energy of docked isoimperatorin and urease complex.

Docking energy	Kcal/mol[a]
Binding energy	−5.70
Ligand efficiency	−0.29
Inhibition constant (μM)	5.99
Intermolecular energy	−6.59
Vdw_hb_desolve_energy	−6.42
Electrostatic energy	−0.18
Torsional energy	−0.89

[a]As measured using AutoDock.

better position in the binding pocket of the targeted protein, with H-bonding at HIS593 and HIS594 residues. The oxygen at position 1 in the compound binds the HIS593 residue with binding distance of 2.80 Å (Figure 2). Similarly, HIS594 binds with the ligand at two positions at a binding distance of 2.3 Å and 3.6 Å. Surprisingly, our isolated compound binds at the same binding pocket near the nickel atoms as reported by Balasubramanian and Ponnuraj (2010). The binding energy value of isoimperatorin (−5.70 kcal/mol) represents its high affinity with the target protein (Table 3). The binding energy value and number of H-bond interactions suggests a high stability for the ligand–protein complex.

Conclusions

The present study demonstrated that isoimperatorin isolated from the roots of *O. koreanum* possess remarkable antiulcer activity in different ulcer models, with the greatest protection against ethanol-induced ulcers. Its jack bean urease inhibitory activity may also translate into the potential to reduce ulceration. The docking results revealed its strong binding affinity with the target protein. Based on our results, isoimperatorin may be used for the development of antiulcer drugs with minimal cytotoxic effects.

Disclosure statement

The authors declare no conflicts of interest.

References

Adam J, Singer MD, Richard AF, Clark MD. 1999. Cutaneous wound healing. N Engl J Med. 341:738–746.

Awaad AS, Al-Rifai AA, El-Meligy RM, Alafeefy AM, Zain ME. 2015. New activities for isolated compounds from convolvulus austro-aegyptiacus as anti-ulcerogenic, anti-helicobacter pylori and their mimic synthesis using bio-guided fractionation. Phytother Res. 29:1311–1316.

Balasubramanian A, Ponnuraj K. 2010. Crystal structure of the first plant urease from Jack bean: 83 years of journey from its first crystal to molecular structure. J Mol Biol. 400:274–283.

Brett D. 2008. A review of collagen and collagen-based wound dressings. Wounds. 20:347–356.

Brzozowski T, Konturek PC, Sliwowski Z, Kwiecien S, Drozdowicz D, Pawlik M, Mach K, Konturek SJ, Pawlik WW. 2006. Interaction of nonsteroidal anti-inflammatory drugs (NSAID) with *Helicobacter pylori* in the stomach of humans and experimental animals. J Physiol Pharmacol. 57:67–79.

Bucciarelli A, Minetti A, Milczakowskyg C, Skliar M. 2010. Evaluation of gastroprotective activity and acute toxicity of *Solidago chilensis* Meyen (Asteraceae). Pharm Biol. 48:1025–1030.

Chen VB, Arendall WB, Headd JJ, Keedy DA, Immormino RM, Kapral GJ, Murray LW, Richardson JS, Richardson DC. 2009. *MolProbity*: all-atom structure validation for macromolecular crystallography. Acta Crystallogr D Biol Crystallogr. 66:12–21.

de Souza Almeida ES, Cechinel Filho V, Niero R, Clasen BK, Balogun SO, de Oliveira Martins DT. 2011. Pharmacological mechanisms underlying the anti-ulcer activity of methanol extract and canthin-6-one of Simaba ferruginea A. St-Hil. in animal models. J Ethnopharmacol. 134:630–636.

Djahanguiri B. 1968. The production of acute gastric ulceration by indomethacin in the rat. Scand J Gastroenterol. 4:265–267.

Fatima AD, Modolo LV, Conegero Sanches AC, Porto RR. 2008. Wound healing agents: the role of natural and non-natural products in drug development. Mini Rev Med Chem. 8:879–888.

Gillessen A, Voss B, Rauterberg J, Domschke W. 1993. Distribution of collagen types I, III, and IV in peptic ulcer and normal gastric mucosa in man. Scand J Gastroenterol. 28:688–689.

Goel RK, Bhattacharya SK. 1991. Gastroduodenal mucosal defence and mucosal protective agents. Indian J Exp Biol. 29:701–714.

Hermes D, Dudek DN, Maria MD, Horta LP, Lima EN, de Fátima Â, Sanches AC, Modolo LV. 2013. *In vivo* wound healing and antiulcer properties of white sweet potato (*Ipomoea batatas*). J Adv Res. 4:411–415.

Ji CX, Fan DS, Li W, Guo L, Liang ZL, Xu RM, Zhang JJ. 2012. Evaluation of the anti-ulcerogenic activity of the antidepressants duloxetine, amitriptyline, fluoxetine and mirtazapine in different models of experimental gastric ulcer in rats. Eur J Pharmacol. 691:46–51.

Kabsch W, Sander C. 1983. Dictionary of protein secondary structure: pattern recognition of hydrogen-bonded and geometrical features. Biopolymers. 22:2577–2637.

Karplus PA, Pearson MA, Hausinger RP. 1997. RP70 years of crystalline urease: what have we learned?. Acc Chem Res. 3:330–337.

Konturek SJ, Konturek PC, Brzozowski T, Konturek JW, Pawlik WW. 2005. From nerves and hormones to bacteria in the stomach; Nobel prize for achievements in gastrology during last century. J Physiol Pharmacol. 56:507–530.

Lovell SC, Davis IW, Arendall WB, de Bakker PI, Word JM, Prisant MG, Richardson JS, Richardson DC. 2003. Structure validation by Calpha geometry: phi,psi and Cbeta deviation. Proteins. 50:437–450.

Malfertheiner P, Chan FK, McColl KE. 2009. Peptic ulcer disease. The Lancet. 374:1449–1461.

Masuda E, Kawano S, Nagano K, Tsuji S, Takei Y, Tsujii M, Oshita M, Michida T, Kobayashi I, Nakama A, et al. 1995. Endogenous nitric oxide modulates ethanol-induced gastric mucosal injury in rats. Gastroenterology. 108:58–64.

Mobley HL, Hausinger RP. 1989. Microbial ureases: significance, regulation, and molecular characterization. Microbiol Rev. 53:85–108.

Morris GM, Huey R, Lindstrom W, Sanner MF, Belew RK, Goodsell DS, Olson AJ. 2009. AutoDock4 and AutoDockTools4: automated docking with selective receptor flexibility. J Comput Chem. 30:2785–2791.

Pettersen EF, Goddard TD, Huang CC, Couch GS, Greenblatt DM, Meng EC, Ferrin TE. 2004. UCSF Chimera-a visualization system for exploratory research and analysis. J Comput Chem. 25:1605–1612.

Pires DE, Blundell TL, Ascher DB. 2015. pkCSM: predicting small-molecule pharmacokinetic and toxicity properties using graph-based signatures. J Med Chem. 58:4066–4072.

Rafiq M, Saleem M, Hanif M, Maqsood MR, Rama NH, Lee KH, Seo SY. 2012. Synthesis and biological activities of some new 3, 6-disubstituted 1, 2, 4-triazolo [3, 4-b] 1, 3, 4-thiadiazole derivatives. Bull Korean Chem Soc. 33:3943–3949.

Rajnikant Gupta VK, Singh A, Lal M, Gupta BD, Banerjee SK. 1996. Crystal structure of isoimperatorin-A furanocoumarin. Mol Cryst Liq Cryst C-Mole Mat. 6:199–203.

Ramakrishnan K, Salinas RC. 2007. Peptic ulcer disease. Am Fam Physicians. 76:1005–1012.

Ramsay KST, Wafo P, Ali Z, Khan A, Oluyemisi OO, Marasini BP, Khan IA, Bonaventure NT, Choudhary MI. 2012. Chemical constituents of *Stereospermum acuminatissimum* and their urease and α-chymotrypsin inhibitions. Fitoterapia. 83:204–208.

Ray WA, Chung CP, Stein CM, Smalley WE, Hall K, Arbogast PG, Griffin MR. 2007. Risk of peptic ulcer hospitalizations in users of NSAIDs with gastroprotective cotherapy versus coxibs. Gastroenterology. 133:790–798.

Santin JR, Lemos M, Júnior LCK, Niero R, de Andrade SF. 2010. Antiulcer effects of *Achyrocline satureoides* (Lam.) DC (Asteraceae) (Marcela), a folk medicine plant, in different experimental models. J Ethnopharmacol. 130:334–339.

Shahin M, Gillessen A, Pohle T, Weber C, Schuppan D, Herbst H, Domschke W. 1997. Gastric ulcer healing in the rat: kinetics and localisation of de novo procollagen synthesis. Gut. 41:187–194.

Shay H. 1945. A simple method for the uniform production of gastric ulceration in the rat. Gastroenterology. 5:43–61.

Sidahmed HM, Hashim NM, Amir J, Abdulla MA, Hadi AHA, Abdelwahab SI, Taha MME, Hassandarvish P, Teh X, Loke MF, et al. 2013. Pyranocycloartobiloxanthone A, a novel gastroprotective compound from *Artocarpus obtusus* Jarret, against ethanol-induced acute gastric ulcer *in vivo*. Phytomedicine. 20:834–843.

Srivastava SK, Nath C, Gupta MB, Vrat S, Sinha JN, Dhawan KN, Gupta GP. 1991. Protection against gastric ulcer by verapamil. Pharmacol Res. 23:81–86.

Studio D. 2008. Version 2.1. Accelrys: San Diego, CA.

Sumbul S, Ahmad MA, Asif M, Akhtar M. 2011. Role of phenolic compounds in peptic ulcer: an overview. J Pharm Bioallied Sci. 3:361–367.

Tsukimi Y, Nakai H, Itoh S, Amagase K, Okabe S. 2001. Involvement of heat shock proteins in the healing of acetic acid-induced gastric ulcers in rats. J Physiol Pharmacol. 52:391–406.

Weatherburn MW. 1967. Enzymic method for urea in urine. Anal Chem. 39:971–974.

Wolfe MM, Lichtenstein DR, Singh G. 1999. Gastrointestinal toxicity of non-steroidal antiinflammatory drugs. N Engl J Med. 340:1888–1899.

Yun WS, Choi BJ, Baek WG, Heo G, Seo YB, Lee JS, Choi HY. 2003. Cluster analysis of Korean Gangwhal by RAPD analysis. Korea J Herbol. 18:141–141.